Tellus (2000), 52B, 239–257
Printed in UK. All rights reserved

TELLUS
ISSN 0280–6509

A comparison of aerosol chemical and optical properties from the 1st and 2nd Aerosol Characterization Experiments

By P. K. QUINN[1,2]*, T. S. BATES[1,2], D. J. COFFMAN[1,2], T. L. MILLER[1,2], J. E. JOHNSON[1,2], D. S. COVERT[1,2], J.-P. PUTAUD[3], C. NEUSÜß[4] and T. NOVAKOV[5], [1]*Pacific Marine Environmental Laboratory, NOAA, 7600 Sand Point Way NE, Seattle, WA 98115, USA;* [2]*Joint Institute for the Study of the Atmosphere and Ocean, University of Washington, Seattle, WA 98195, USA;* [3]*Environment Institute (JRC), European Commission, Ispra, Italy;* [4]*Institute for Tropospheric Research, Permoserstr 15, Leipzig D, 04303, Germany;* [5]*Lawrence Berkeley National Laboratory, Berkeley, CA 94720, USA*

(Manuscript received 4 February 1999; in final form 13 September 1999)

ABSTRACT

Shipboard measurements of aerosol chemical composition and optical properties were made during both ACE-1 and ACE-2. ACE-1 focused on remote marine aerosol minimally perturbed by continental sources. ACE-2 studied the outflow of European aerosol into the NE Atlantic atmosphere. A variety of air masses were sampled during ACE-2 including Atlantic, polar, Iberian Peninsula, Mediterranean, and Western European. Reported here are mass size distributions of non-sea salt (nss) sulfate, sea salt, and methanesulfonate and submicron and supermicron concentrations of black and organic carbon. Optical parameters include submicron and supermicron aerosol scattering and backscattering coefficients at 550 nm, the absorption coefficient at 550 ± 20 nm, the Ångström exponent for the 550 and 700 nm wavelength pair, and single scattering albedo at 550 nm. All data are reported at the measurement relative humidity of 55%. Measured concentrations of nss sulfate aerosol indicate that, relative to ACE-1, ACE-2 aerosol during both marine and continental flow was impacted by continental sources. Thus, while sea salt controlled the aerosol chemical composition and optical properties of both the submicron and supermicron aerosol during ACE-1, it played a relatively smaller role in ACE-2. This is confirmed by the larger average Ångström exponent for ACE-2 continental aerosol of 1.2 ± 0.26 compared to the ACE-1 average of -0.03 ± 0.38. The depletion of chloride from sea salt aerosol in ACE-2 continental air masses averaged $55 \pm 25\%$ over all particle sizes. This compares to the ACE-2 marine average of $4.8 \pm 18\%$ and indicates the enhanced interaction of anthropogenic acids with sea salt as continental air masses are transported into the marine atmosphere. Single scattering albedos averaged 0.95 ± 0.03 for ACE-2 continental air masses. Averages for ACE-2 and ACE-1 marine air masses were 0.98 ± 0.01 and 0.99 ± 0.01, respectively.

1. Introduction

The Aerosol Characterization Experiments (ACE) are designed, in part, to reduce the uncertainty of aerosol radiative forcing estimates by quantifying relevant aerosol properties and processes. To determine the radiative forcing resulting from anthropogenic aerosol, the optical properties and factors controlling them must be well defined for both the anthropogenic and natural background aerosol. ACE-1 focused on the properties of a natural marine aerosol system (Bates et al., 1998). It took place in November and December

* Corresponding author.
e-mail: quinn@pmel.noaa.gov.

of 1995 in the Southern Ocean environment south of Australia and west of Tasmania, a region minimally perturbed by anthropogenic and continental aerosol sources. ACE-2 focused on pollution aerosol as it was transported from Europe into the marine atmosphere (Verver et al., 2000). It was conducted in June and July of 1997 over the northeast Atlantic Ocean in the region roughly bounded by Portugal, Tenerife, and the Azores.

Meteorology in the ACE-1 region during November and December is typified by frequent frontal passages. During the experiment, 14 cold fronts and 1 warm front passed through the ACE-1 region so that every few days there was a marked change in synoptic conditions (Hainsworth et al., 1998). During November there was greater than usual west to northwesterly flow and less north-south transport. As a result, there was some flow and mixing of relatively unpolluted continental air from Australia into the marine westerlies south of Australia. During December, south to southwesterly flow dominated bringing air masses which had spent 10 or more days over the ocean into the region. ^{222}Rn concentrations were less than 100 mBq m^{-3} for most of the experiment with a few short-lived increases to 600 mBq m^{-3} lasting from 7 to 13 h, indicating that for both flow regimes, sampled air masses were relatively free of continental influences (Whittlestone et al., 1998).

Air mass transport in the ACE-2 region is controlled by the location of the Azores High (Raes et al., 2000). When located west of the Azores, flow around the northern edge of the anticyclone brings maritime air into the ACE-2 region. After the passage of a cold front at mid-latitudes, the high can extend into Western Europe resulting in the transport of polluted air from Europe into the ACE-2 region. Air mass back trajectories indicate that air masses flowed from 5 regions during ACE-2 (Fig. 1). Marine air masses came from over the Atlantic or north of the Arctic circle (denoted here as polar). Continental air masses flowed from the Iberian Peninsula, the Mediterranean, or Western Europe. ^{222}Rn concentrations during continental flow reached levels near 8000 mBq m^{-3}, indicating the greater degree of continental influence in the ACE-2 than the ACE-1 region.

During both ACE-1 and ACE-2, shipboard measurements were made of aerosol chemical and optical properties including chemical mass size

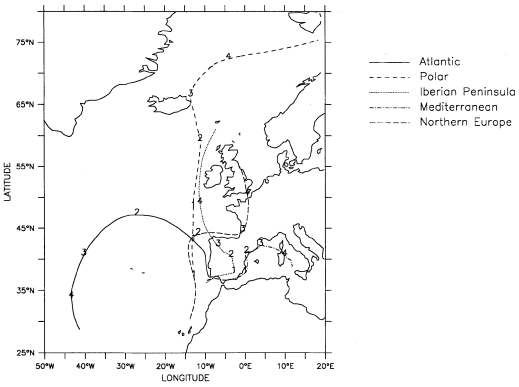

Fig. 1. ACE-2 study region and example air mass back trajectories showing the flow that occurred from different regions during the experiment. Numbers represent days back in time. Trajectories end at the ship's position.

distributions and aerosol scattering, backscattering, and absorption coefficients. Results from the ACE-1 measurements have been reported in detail in Quinn et al. (1998). This paper will focus primarily on results from measurements taken onboard the *RV Vodyanitskiy* during ACE-2 but will also include comparisons with the clean marine case of ACE-1. Specific chemical parameters include the mass size distribution of non-sea salt (nss) sulfate and sea salt aerosol and concentrations of submicron and supermicron carbonaceous aerosol. Optical parameters include submicron and supermicron aerosol scattering and backscattering coefficients at 550 nm, the absorption coefficient at 550 ± 20 nm, the Ångström exponent for the 550 and 700 nm wavelength pair, and single scattering albedo at 550 nm. In addition, comparisons will be made to two land-based ACE-2 stations to assess variability in the region's aerosol chemical composition. These are Sagres (37°N, 8.9°W) located at the outermost SW tip of Portugal and Punta del Hildalgo (28.6°N, 16.3°W) located on the NE tip of Tenerife.

Aerosol physical properties measured onboard the *RV Vodyanitskiy* and the processes controlling them are discussed in a companion paper by Bates et al. (2000). An extensive discussion of shipboard carbonaceous aerosol measurements is presented by Novakov et al. (2000). Further details of measurements of chemical composition measured at Sagres and Punta del Hildalgo can be found in

Neusüß et al. (2000) and Putaud et al. (2000), respectively.

2. ACE-2 measurements

2.1. Aerosol sample inlet

Sample air for the chemical and optical measurements was drawn through a 6-m sample mast. The entrance to the mast was 10 m above sea level and forward of the ship's stack. To maintain nominally isokinetic flow and minimize the loss of supermicron particles, the inlet was rotated into the relative wind. Air entered the inlet through a 5-cm diameter hole, passed through an expansion cone, and then into the 20-cm diameter sampling mast. The flow through the mast was 1 m^3 min^{-1}. The last 1.5 m of the mast were heated to establish a stable reference relative humidity (RH) for the sample air of about 55%. This allows for constant instrumental size segregation in spite of variations in ambient RH. Individual 1.9 cm diameter stainless steel tubes extended into the heated portion of the mast. These were connected to the aerosol instrumentation with graphite-polyethylene conductive tubing to prevent the electrostatic loss of particles. An exception to this was the lines connected to the impactors used for collection of carbonaceous aerosol; they were constructed of stainless steel. Air was sampled only when the concentration of particles greater than 15 nm in diameter indicated the sample air was free of contamination, the relative wind speed was greater than 3 m s^{-1}, and the relative wind was forward of the beam.

2.2. Chemical mass size distributions of the major ions

Seven-stage multi-jet cascade impactors (Berner et al., 1979) sampling air at 55% RH were used to determine the mass size distributions of Cl^-, Br^-, NO_3^-, $SO_4^=$, methanesulfonate (MSA^-), Na^+, NH_4^+, K^+, Mg^{+2}, and Ca^{+2}. The RH of the sampled air stream was measured a few inches upstream from the impactor. The 50% aerodynamic cutoff diameters, $D_{50,aero}$, were 0.18, 0.31, 0.55, 1.1, 2.0, 4.1, and 10 μm. Throughout the paper submicron refers to particles with $D_{50,aero} < 1.1$ μm at 55% RH and supermicron refers to particles with 1.1 μm $< D_{50,aero} < 10$ μm at 55% RH.

The impaction stage at the inlet of the impactor was coated with silicone grease to prevent the bounce of larger particles onto the downstream stages. Tedlar films were used as the collection substrate in the impaction stages and a Millipore Fluoropore filter (1.0-μm pore size) was used for the backup filter. Films were cleaned in an ultrasonic bath in 10% H_2O_2 for 30 min, rinsed in distilled, deionized water, and dried in an NH_3- and SO_2-free glove box. All handling of the substrates was done in the glove box. Blank levels were determined by loading an impactor with substrates but not drawing any air through it.

Non-sea salt sulfate concentrations were calculated from Na^+ concentrations and the ratio of sulfate to sodium in seawater. Sea salt aerosol concentrations were calculated as

$$\text{sea salt } (\mu g\, m^{-3}) = Cl^- (\mu g\, m^{-3}) + Na^+ (\mu g\, m^{-3}) \times 1.47, \quad (1)$$

where 1.47 is the seawater ratio of $(Na^+ + K^+ + Mg^{+2} + Ca^{+2} + SO_4^= + HCO_3^-)/Na^+$ (Holland, 1978). This approach prevents the inclusion of non-seasalt K^+, Mg^{+2}, Ca^{+2}, $SO_4^=$, and HCO_3^- in the sea salt mass and allows for the loss of Cl^- mass through Cl^- depletion processes. It also assumes that all measured Na^+ is derived from seawater.

Concentrations of the aerosol chemical components are given in units of μg m^{-3}. Factors for converting from μg m^{-3} to volume mixing ratios (at 25°C and 1 atm) are given in Tables 1 and 2.

2.3. Submicron and supermicron carbonaceous aerosol concentrations

Two-stage multi-jet cascade impactors (Berner et al., 1979) sampling air at 55% RH were used to determine submicron and supermicron concentrations of total, organic, and black carbon. The impactor had $D_{50,aero}$ of 1.1 and 10 μm. Supermicron particles were collected on an Al foil and submicron particles on a quartz filter. The impactor also included a second backup quartz filter to assess positive artifacts associated with collecting gas phase organic species. The Al foils and quartz filters were heated immediately before use at 600°C for 4 h to remove organic contaminants. Blank levels were determined by placing

Table 1. *Submicron aerosol chemical composition as a function of air mass origin and comparison to ACE-1, Sagres and PdH*

Air mass origin	N[a]	Sea salt[b] ($\mu g\ m^{-3}$)	Nss sulfate[c] ion ($\mu g\ m^{-3}$)	Nss sulfate[d] aerosol ($\mu g\ m^{-3}$)	NH_4/nss SO_4 molar ratio	MSA[e] ($\mu g\ m^{-3}$)	MSA/nss SO_4 molar ratio	BC[f] ($\mu g\ C\ m^{-3}$)	OC[g] ($\mu g\ C\ m^{-3}$)
Atlantic	4(0)	0.60 ± 0.51 (8.3 ± 2.2)	0.68 ± 0.17	0.74 ± 0.20	0.51 ± 0.13	0.08 ± 0.05	0.11 ± 0.04	NA	NA
Polar	4(0)	0.42 ± 0.28 (6.4 ± 2.5)	0.62 ± 0.12	0.67 ± 0.12	0.50 ± 0.12	0.08 ± 0.01	0.14 ± 0.02	NA	NA
Iberian Peninsula	18(6)	0.88 ± 1.5 (8.5 ± 1.9)	6.8 ± 2.0	7.9 ± 2.4	0.85 ± 0.25	0.09 ± 0.06	0.02 ± 0.02	0.40 ± 0.20	0.69 ± 0.29
Mediterranean	3(1)	0.34 ± 0.05 (6.9 ± 2.0)	5.3 ± 1.7	6.6 ± 1.8	1.5 ± 0.63	0.11 ± 0.04	0.02 ± 0.003	1.1	2.8
Western Europe	4(0)	0.40 ± 0.28 (11 ± 1.6)	6.3 ± 1.5	7.7 ± 1.9	1.1 ± 0.28	0.06 ± 0.04	0.01 ± 0.006	NA	NA
ACE-1	22(0)	1.0 ± 0.55 (9.5 ± 3.8)	0.16 ± 0.06	0.19 ± 0.06	0.67 ± 0.22	0.04 ± 0.03	0.22 ± 0.15	NA	NA
Sagres — clean	5	0.37 ± 0.14	0.43 ± 0.09	0.56 ± 0.13	1.5 ± 0.15	0.02 ± 0.01	0.03 ± 0.07	0.03 ± 0.04	0.07 ± 0.07
Sagres – polluted	7	0.40 ± 0.10	8.8 ± 2.1	11 ± 2.4	1.6 ± 0.61	0.05 ± 0.06	0.01 ± 0.01	0.30 ± 0.08	0.75 ± 32
PdH[h] — clean	24	0.23 ± 0.17	0.35 ± 0.20	0.45 ± 0.25	1.4 ± 0.52	0.02 ± 0.01	0.05 ± 0.02	0.01 ± 0.02	0.14 ± 0.12
PdH — polluted	19	0.24 ± 0.13	3.5 ± 2.0	4.5 ± 2.6	1.6 ± 0.13	0.04 ± 0.01	0.01 ± 0.01	0.11 ± 0.08	0.52 ± 0.27

[a] Number of ion samples (number of carbon samples).
[b] (Wind speed, $m\ s^{-1}$).
[c] $1\ \mu g\ m^{-3}$ nss $SO_4^{=}$ ion = 0.25 ppbv at 25°C and 1 atm.
[d] Nss sulfate aerosol = nss $SO_4^{=} + NH_4^{+}$.
[e] $1\ \mu g\ m^{-3}$ MSA = 0.25 ppbv at 25°C and 1 atm.
[f] BC = black carbon, $1\ \mu g\ m^{-3}$ C = 2.0 ppbv at 25°C and 1 atm.
[g] OC = Organic Carbon, $1\ \mu g\ m^{-3}$ C = 2.0 ppbv at 25°C and 1 atm.
[h] PdH = Punta del Hildalgo.
NA = not available.

Table 2. *Supermicron aerosol chemical composition as a function of air mass origin and comparison to ACE-1, Sagres and PdH*

Air mass origin	N[a]	SO_2 (ppbv)	Sea salt[b] ($\mu g\ m^{-3}$)	Nss sulfate[c] ion ($\mu g\ m^{-3}$)	MSA[d] ($\mu g\ m^{-3}$)	MSA/nss SO_4 molar ratio	BC[e] ($\mu g\ C\ m^{-3}$)	OC[f] ($\mu g\ C\ m^{-3}$)	TC[g] ($\mu g\ C\ m^{-3}$)
Atlantic	4(0)	DL to <0.5	6.3 ± 1.6 (8.3 ± 2.2)	0.15 ± 0.03	0.07 ± 0.07	0.41 ± 0.34	NA	NA	NA
polar	4(0)	DL to <0.34	5.1 ± 2.2 (6.4 ± 2.5)	0.06 ± 0.01	0.09 ± 0.05	0.93 ± 0.19*	NA	NA	NA
Iberian Peninsula	18(6)	DL to <10	10 ± 3.1 (8.5 ± 1.9)	0.66 ± 0.45	0.02 ± 0.02	0.05 ± 0.06	NA	NA	0.87 ± 0.24
Mediterranean	3(1)	0.25 to 1.8	4.2 ± 3.1 (6.9 ± 2.0)	0.22 ± 0.01	0.01 ± 0.01	0.03 ± 0.06	NA	NA	0.96
Western Europe	4(0)	DL to <0.59	9.4 ± 2.2 (11 ± 1.6)	0.37 ± 0.23	0.01 ± 0.02	0.06 ± 0.09	NA	NA	NA
ACE-1	22(0)		9.4 ± 5.5 (9.5 ± 3.8)	0.07 ± 0.09	0.01 ± 0.01	0.63 ± 0.77	NA	NA	NA
Sagres — clean	5		3.9 ± 0.47	0.02 ± 0.03	0.01 ± 0.02	0.38 ± 0.77	0.02 ± 0.03	0.15 ± 0.19	0.17
Sagres — polluted	7		4.8 ± 1.2	0.67 ± 0.37	0.01 ± 0.01	0.01 ± 0.02	0.07 ± 0.03	0.43 ± 0.10	0.50
PdH[h] — clean	24		6.6 ± 2.9	0.04 ± 0.05	0.02 ± 0.01	0.5 ± 0.3	0.02 ± 0.05	0.14 ± 0.16	0.16
PdH — polluted	19		9.1 ± 4.5	0.5 ± 0.38	0.01 ± 0.01	0.06 ± 0.15	0.03 ± 0.03	0.33 ± 0.22	0.36

[a] Number of ion samples (Number of carbon samples).
[b] (Wind speed, $m\ s^{-1}$).
[c] $1\ \mu g\ m^{-3}$ nss $SO_4^=$ ion = 0.25 ppbv at 25°C and 1 atm.
[d] $1\ \mu g\ m^{-3}$ MSA = 0.25 ppbv at 25°C and 1 atm.
[e] BC = Black Carbon, $1\ \mu g\ m^{-3}$ C = 2.0 ppbv at 25°C and 1 atm.
[f] OC = Organic Carbon, $1\ \mu g\ m^{-3}$ C = 2.0 ppbv at 25°C and 1 atm.
[g] TC = Total carbon = black plus organic carbon, $1\ \mu g\ m^{-3}$ C = 2.0 ppbv at 25°C and 1 atm.
[h] PdH = Punta del Hildalgo.
DL = detection limit of 0.1 ppbv. NA = not available.
*Excludes outlier value of 4.25. With outlier value, ratio is 1.8 ± 1.7.

substrates into a second impactor and deploying the impactor for the duration of the sampling period without drawing air through it. Foils and filters were stored frozen in capped glass vials until analysis.

The samples were analyzed by a thermal-evolved gas analysis (EGA) method (Novakov, 1981; Novakov et al., 2000) where the substrates are heated progressively and the evolved gases are converted to CO_2 and analyzed by a non-dispersive infrared analyzer. The reproducibility of this method for total C is $\pm 10\%$. The uncertainties associated with positive and negative sampling artifacts can be substantial. An effort was made to correct for positive artifacts due to the absorption of gas phase organics as follows. The concentration of organic carbon on the backup quartz filter was presumed to be due to the collection of gas phase organic species and was subtracted from the concentration on the front filter.

2.4. *Aerosol scattering, backscattering, and absorption coefficients.*

Measurements of aerosol scattering and hemispheric backscattering coefficients were made with an integrating nephelometer (Model 3563, TSI Inc.) at wavelengths of 450, 550, and 700 nm at 55% RH. The RH was measured inside the nephelometer sensing volume. Two single-stage cascade impactors, one having a $D_{50,\mathrm{aero}}$ of 1.1 μm and the other 10 μm, were placed upstream of the nephelometer. A valve switched between the two impactors every 15 min so that sampling alternated between submicron aerosol and sub-10 μm aerosol. Scattering and backscattering by the supermicron aerosol was determined by difference.

The absorption coefficient for sub-10μm aerosol was measured at 550 ± 20 nm at 55% RH by monitoring the change in transmission through a filter with a Particle Soot Absorption Photometer (PSAP, Radiance Research). Laboratory tests indicate that the PSAP is subject to a small (1 to 1.5%) positive artifact due to instrumental interpretation of scattering as absorption. Measured scattering values at 550 nm and an empirically-derived correction factor were used to correct for this artifact (T. Anderson, personal communication).

The scattering, backscattering, and absorption coefficients were measured at 55% RH and are reported at this reference RH.

2.5. *SO_2*

SO_2 was measured with a pulsed fluorescence SO_2 analyzer (TECO) with a detection limit of 0.1 ppbv. Data were filtered to eliminate periods of calibration, zero, and local contamination when the wind was abaft the beam or when other ships were upwind. Further details are reported by Bates et al. (2000).

2.6. *Ancillary parameters*

Also measured were meteorological parameters including surface temperature, RH, wind speed and direction, as well as vertical profiles of these parameters from radiosondes. Air mass back trajectories were calculated four times daily using the hybrid single-particle Lagrangian integrated trajectory model HY-SPLIT 4 (Draxler, 1992). It is based on wind fields generated by the medium-range forecast model (MRF). ^{222}Rn concentrations were measured using the method of Whittlestone and Zahorowski (1998).

2.7. *Air mass classification*

Shipboard impactor samples were classified as marine or continental based on trajectory analysis, the occurrence of a bimodal aerosol number size distribution, and ^{222}Rn concentrations. In addition, periods of local ship contamination, from either the *Vodyanitskiy* or ships upwind, were identified by rapid increases in the aerosol light absorption coefficient and particle concentration. Samples that included these time periods were omitted from the data analysis.

Sagres impactor samples were classified as marine or continental based on trajectory analysis, local wind direction, the aerosol absorption coefficient, and NO_x and SO_2 concentrations (Neusüß et al., 2000). Periods of contamination by local sources were identified from the local wind direction and spikes in the aerosol absorption coefficient, NO_x and SO_2. Punta del Hildalgo impactor samples were classified as marine or continental based on trajectory analysis and the aerosol absorption coefficient (Putaud et al., 2000).

3. Air mass history during ACE-2

Based on back trajectories the ship was exposed to air masses from five regions during ACE-2: the central north Atlantic, the Atlantic northward of the Arctic Circle (polar), the Iberian Peninsula, the Mediterranean, and Western Europe (Fig. 1). Atlantic flow was sampled with the impactors approximately 18% of the time, Polar flow 10%, Iberian Peninsula flow 42%, Mediterranean flow 5%, and Western European flow 13% of the time. During the remaining 12% of the experiment the air mass history was not well defined as trajectories came from two or more regions over the course of an impactor sampling period. Results from these mixed trajectory time periods have been omitted from the data analysis.

Atlantic flow reached the ship three times during the experiment (day of year 173.0 to 174.7 (22–23 June), 177.6 to 178.5 (26–27 June), and 185 to 186.25 (4–5 July)) and polar flow two times (178.6 to 181.4 (27–30 June) and 183.8 to 185.0 (2–3 July)) (Fig. 2). (Here, day of year is defined so that 1 January at noon is 1.5). Both types of marine flow resulted from the presence of a low pressure system over western Europe. The location of the Icelandic Low as well as the Azores High affected whether the flow was Atlantic or polar. During these periods boundary layer depths ranged from 800 to 3300 m. Larger boundary layer depths occurred before and/or after the passage of frontal systems. Back trajectories indicate that during periods of Atlantic flow, air occasionally subsided from the upper troposphere several days before reaching the ship. Large scale, weak subsidence was a consistent feature during polar flow.

Flow from the Iberian Peninsula to the ship occurred 5 times (174.7 to 176.7 (23–25 June), 183.0 to 183.8 (2 July), 186.3 to 187.3 (5–6 July), 188.75 to 189.5 (7–8 July), and 193.5 to 201.2 (12–20 July)). The high over the Azores and a low over Europe were positioned such that flow from the east-northeast brought air from the Iberian Peninsula to the ship. In all cases there was a well-defined boundary layer ranging from 300 to 2500 m. During these 5 periods, the ship's position ranged from the Portuguese coast near Sagres to 600 km offshore. During the longest period of Iberian flow (193.5 to 201.2), the ship was within 200 km of the coast but moved from 33°N to 40°N. Based on the ship's distance from the coast and back trajectories, transport times from sources along the coast ranged from a fraction of a day to, at most, 2 days. The changing position of the ship relative to the location of the high pressure system contributed to variability observed in the measured aerosol properties. Additional variability during the 193.5 to 201.2 time period may have resulted from subsidence of upper tropospheric air to the surface 3 to 4 days before the sampled air reached the ship.

Flow from the Mediterranean to the ship occurred only once (187.3 to 188.75 (6–7 July)). During this time, the ship initially was located near Sagres. It then moved south from 36.6°N to 33.8°N and west from 10°W to 11.6°W, essentially due west from the entrance to the Strait of Gibraltar. Back trajectories indicate that the sampled air was over the Mediterranean less than 24 h before reaching the ship. Vertical profiles of relative humidity indicate that there was a very shallow boundary layer (<100 m) over the ship during this period. Most likely, the associated inversion was established only a few hours upwind of the ship as the continental air mass reached the cold water. Prior to this, mixing between the upper troposphere and the surface could have occurred. Based on shipboard lidar profiles, however, the upper troposphere (up to 6 km) did not appear to be a strong aerosol source relative to aerosol concentrations measured at the surface (V. Freudenthaler, pers. commun.).

There were two periods of flow from Western Europe (189.5 to 192.5 (8–11 July) and 202.35 to 203.21 (21–22 July)). During the first, a ridge of high pressure stretched across the North Atlantic and extended over France so that flow from the northeast brought European air just west of the Iberian Peninsula and south over the ocean to the ship. The ship was transiting from 34°N to 29°N between 15°W and 12°W. During the second period, a high pressure system extended from the Azores to the North Sea again resulting in flow of European air over the Atlantic. Initially air flowed from over the Iberian Peninsula as the ship was transiting between 34N and 40°N (193.5 to 201.25). Once the ship remained in the more confined region near 40.5°N and 11°W, air flowed from Western Europe (202.35 to 203.21). During both periods boundary layer heights were between 400 and 900 m. Back trajectories indicate that, during the earlier period, subsidence of air from

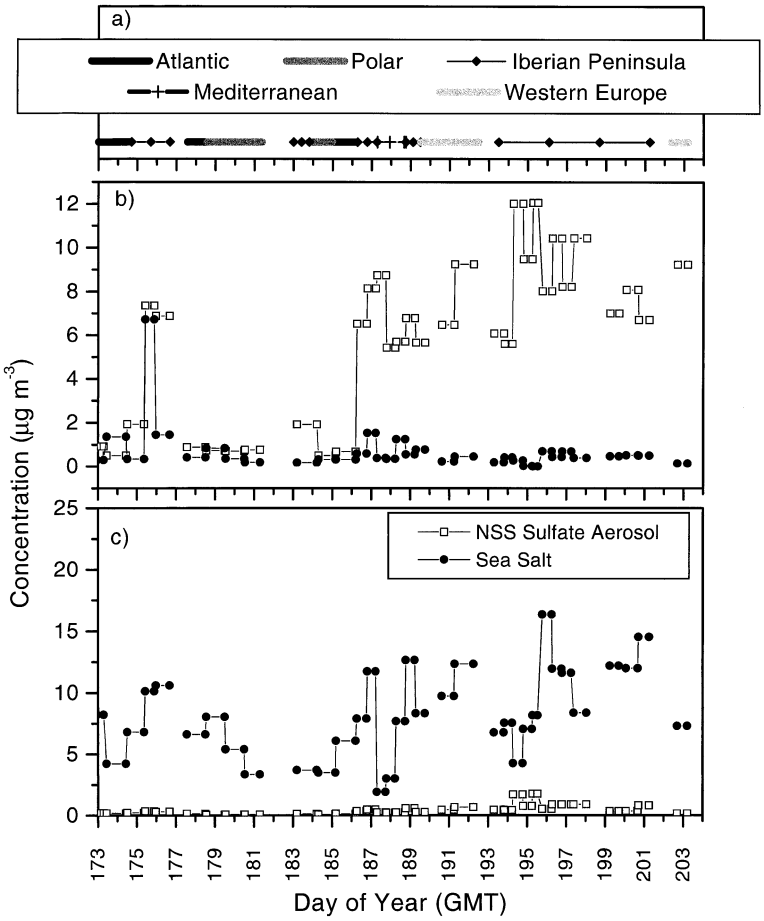

Fig. 2. Shown as a function of day of year throughout the experiment are (a) air mass flow (gaps represent time periods of mixed trajectories), (b) submicron nss sulfate aerosol (includes nss $SO_4^=$ and NH_4^+) and sea salt aerosol concentration and (c) supermicron nss sulfate and sea salt aerosol concentration.

the free troposphere occurred 3 to 4 days before the sampled air reached the ship. Depending on the position of the ship, there was a 2 to 6 day transport time within the boundary layer from Western Europe to the ship.

During ACE-2, there were three outbreaks of pollution from the European continent that were observed throughout the ACE-2 domain (Raes et al., 2000). There were other cases, however, where pollution was observed at Sagres and on the ship but not at Punta del Hildago. In addition, there were instances where Sagres observed pollution from the Mediterranean while Punta del Hildalgo observed pollution from the Western European coast. This complexity of air mass history makes pseudo-Lagrangian comparisons of the aerosol chemical composition observed at Sagres, the ship, and Punta del Hildalgo difficult. As a result, comparisons between the three platforms are made to assess regional differences that were observed as a function of air mass type rather than track the evolution of the aerosol in a Lagrangian framework.

4. Results — aerosol chemical composition

4.1. Nss sulfate aerosol

Submicron nss sulfate aerosol (which includes both nss $SO_4^=$ and associated NH_4^+) concentra-

tions measured in marine air masses were, on average, an order of magnitude lower than continental values with no significant difference between Atlantic and polar air masses (Fig. 2, Table 1). In addition, concentrations at the ship were within the range of marine concentrations from Sagres and Punta del Hildalgo. These marine values were, however, almost 4 × greater than those measured during ACE-1. The calculated ocean to atmosphere flux of dimethylsulfide was comparable for ACE-1 and ACE-2 (Bates et al., 2000) suggesting that the biogenic source of nss $SO_4^=$ was similar for the two experiments. Assuming that upwind DMS fluxes were similar for both experiments, the larger concentrations of nss sulfate aerosol measured during ACE-2 indicate the degree to which anthropogenic sources from North America or Europe impact the NE Atlantic even under conditions of marine flow.

Nss sulfate aerosol concentrations were similar for the three continental air masses but average size distributions were slightly different (Fig. 3b). Of the three regions, the Mediterranean had the highest average concentration on the first two impactor stages (1.1 ± 0.59 μg m^{-3} and 1.5 ± 0.25 μg m^{-3}) while Western Europe had the lowest average concentration in this size range (0.24 ± 0.08 μg m^{-3} and 1.1 ± 0.20 μg m^{-3}). This trend reversed on the third and fourth impactor stages such that the Mediterranean samples had the lowest average concentration (2.9 ± 1.3 μg m^{-3} and 1.2 ± 0.34 μg m^{-3}) and Western European air masses had the highest (4.3 ± 0.81 μg m^{-3} and 2.0 ± 0.98 μg m^{-3}). These differences, though slight, could be due to the length of time the aerosol spent in the boundary layer prior to being sampled on the ship (denoted here as aerosol boundary layer residence time). A longer transport time in the boundary layer allows for the deposition of gas phase species onto particles and the passage of particles through clouds. Both of these mechanisms result in particle growth (Hegg et al., 1992; Hoppel et al., 1994). Aerosol originating near the Mediterranean would have spent the shortest amount of time in transit in the boundary layer (less than one day) while aerosol from the Iberian Peninsula and Western Europe would have spent up to 2 days and 2 to 6 days in transit, respectively. It also may be that aerosol collected during Mediterranean flow originated upwind of the Mediterranean but experienced relatively less cloud processing while en route to the ship compared to aerosol from the other continental regions. METEOSAT visible images (1200 GMT) indicate clear skies along the trajectory 3 to 4 days upwind of the ship (3–7 July) with scattered clouds occurring only on 4 July. Based on shipboard observations, the average cloud cover during the period of Mediterranean flow was 6% compared to approximately 60% during the rest of the experiment.

The submicron nss $SO_4^=$ aerosol concentration during continental flow on the ship averaged 7.7 ± 2.2 μg m^{-3}. The continental average measured at Sagres was a factor of 1.5 higher than this while the average at Punta del Hildalgo was about a factor of 1.5 lower (Table 1). During the first period of Western European flow (189 to 192, 8–11 July), the submicron nss $SO_4^=$ aerosol concentration on the ship was 7.1 ± 1.9 μg m^{-3} and at Sagres was 10 ± 3.3 μg m^{-3}. Values at Punta del Hildalgo during this same period averaged 3.5 ± 0.75 μg m^{-3}. The general trend in a decrease in concentration from Sagres to the ship to Punta del Hildalgo may be a result of the increase in transport time from Europe and the corresponding dilution of the continental plume and deposition of submicron aerosol. On day 190 (9 July), the ship was located near 30.5°N and 14°W which, according to trajectories, was about 2 days further downwind from Western Europe than Sagres was. Punta del Hildalgo was approximately one day downwind of the ship. Local sources near Sagres do not appear to have contributed to the higher submicron nss $SO_4^=$ aerosol concentrations. This is based on a northwesterly local wind, a very stable aerosol absorption coefficient over the several day period, and NO_x and SO_2 concentrations comparable to those observed during marine flow. Unfortunately, no gas phase anthropogenic tracer such as CO was measured at all three platforms to provide evidence for the transport and dilution hypothesis.

As can be seen in Figs. 3a, b, very little nss $SO_4^=$ aerosol was found in the supermicron size range. The average ratio of the supermicron to total (submicron plus supermicron) nss $SO_4^=$ aerosol mass concentration for the experiment was 0.09 ± 0.05. Supermicron nss $SO_4^=$ concentrations appear to be a function of both the SO_2 and supermicron sea salt aerosol concentration with higher values corresponding to air masses with

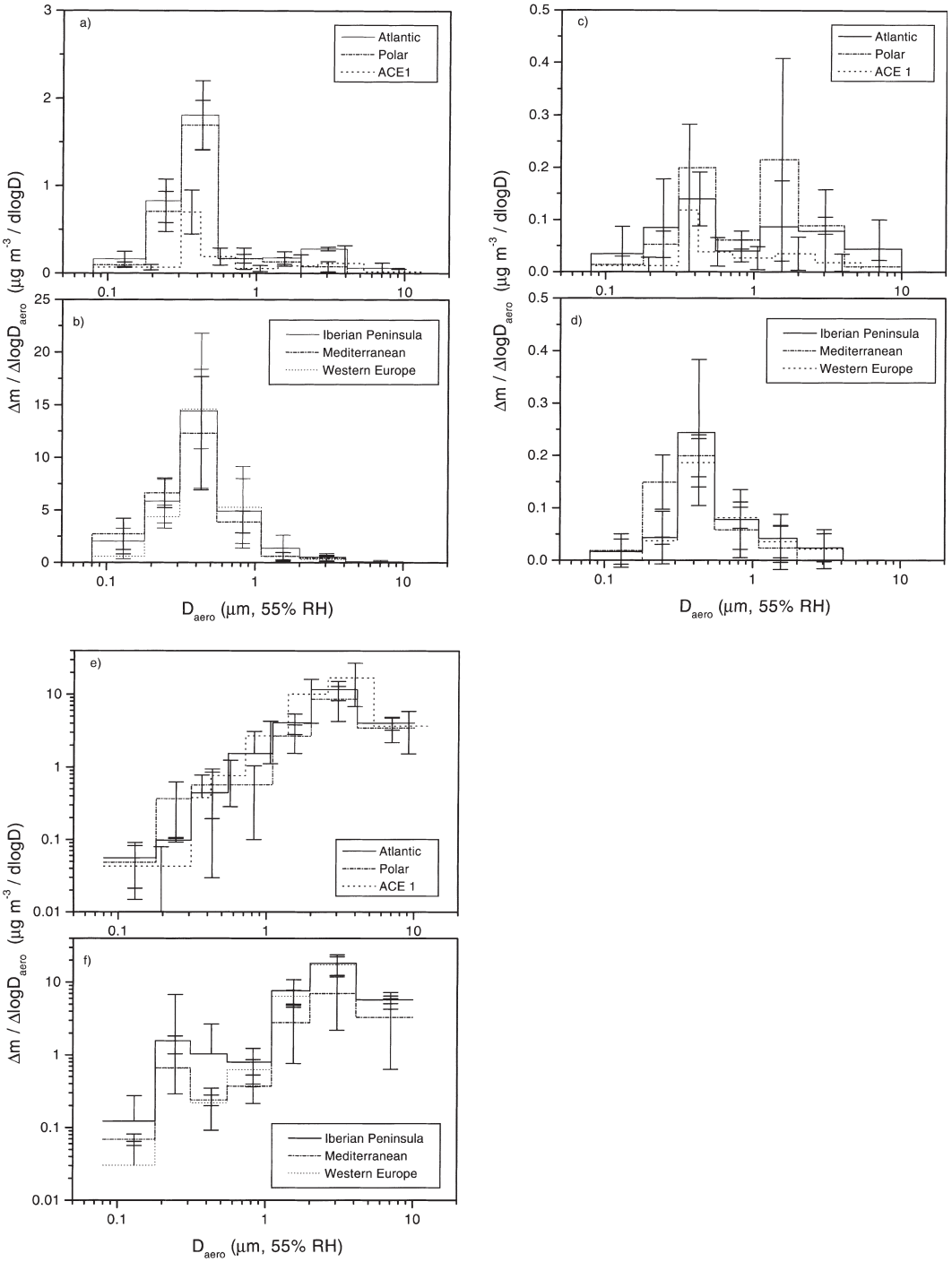

Fig. 3. Average mass size distribution plotted as $\Delta m/\Delta \log D_{aero}$ versus log of D_{aero} at 55% RH for (a) marine and (b) continental nss $SO_4^=$ aerosol (includes nss $SO_4^=$ and NH_4^+), (c) marine and (d) continental MSA^- and (e) marine and (f) continental sea salt aerosol.

higher SO_2 and supermicron sea salt concentrations. The marine samples had the lowest supermicron nss $SO_4^=$ values corresponding to relatively low SO_2 concentrations. Of the continental air masses, samples from the Iberian Peninsula had the highest supermicron nss $SO_4^=$ concentrations corresponding to both high SO_2 and supermicron sea salt concentrations.

A comparison of supermicron nss $SO_4^=$ aerosol concentrations from Sagres, the ship, and Punta del Hildalgo for the first period of Western European flow shows a similar result as for the submicron size range. Average concentrations decrease from Sagres (0.61 ± 0.53 μg m^{-3}) to the ship (0.45 ± 0.20 μg m^{-3}) to Punta del Hildalgo (0.29 ± 0.10 μg m^{-3}).

Submicron NH_4^+ to nss $SO_4^=$ molar ratios averaged around 0.5 for both Atlantic and polar air masses. A molar ratio less than or equal to 1 is typical for marine regions where there is insufficient NH_3 to fully neutralize the sulfate aerosol (Quinn et al., 1988; Covert, 1988). Continental sources of NH_3 are much larger than marine sources (Dentener and Crutzen, 1994). This is confirmed by the higher ratios observed for the three continental regions (0.85 for the Iberian Peninsula, 1.5 for the Mediterranean, and 1.1 for Western Europe). Still, the sulfate aerosol was not fully neutralized by ammonia suggesting a molecular composition of NH_4HSO_4 rather than $(NH_4)_2SO_4$. The supermicron NH_4^+ to nss $SO_4^=$ molar ratio was much lower averaging 0.07 ± 0.18. This agrees with previously reported observations from the northeast Atlantic (Huebert et al., 1996) and indicates that most ammonia condensed upon existing submicron particles so that very little was associated with supermicron nss $SO_4^=$.

4.2. *Methanesulfonate*

Submicron MSA^- concentrations were similar for all air masses (Table 1). The Atlantic and polar air masses averaged 0.08 ± 0.05 μg m^{-3} and 0.08 ± 0.01 μg m^{-3} respectively. Average values from the Iberian Peninsula, the Mediterranean, and Western Europe were 0.09 ± 0.06 μg m^{-3}, 0.11 ± 0.04 μg m^{-3}, and 0.06 ± 0.04 μg m^{-3}, respectively. Larger differences were observed in the supermicron concentrations. For the marine regions, average supermicron concentrations were comparable to submicron values (0.07 ± 0.07 μg m^{-3} and 0.09 ± 0.05 μg m^{-3} for Atlantic and polar air masses, respectively) yielding bimodal MSA^- size distributions (Fig. 3c). Continental supermicron concentrations were considerably less. Average values for the Iberian Peninsula, the Mediterranean, and Western Europe were 0.02 ± 0.02 μg m^{-3}, 0.01 ± 0.01 μg m^{-3}, and 0.01 ± 0.02 μg m^{-3}, respectively. Hence, the continental size distributions were monomodal (Fig. 3d) and similar to the shape of the nss sulfate aerosol size distributions.

Submicron ACE-1 MSA^- concentrations were slightly lower than those observed during ACE-2 averaging 0.04 ± 0.03 μg m^{-3}. Supermicron concentrations were significantly lower than ACE-2 marine supermicron concentrations averaging 0.01 ± 0.01 μg m^{-3}. Hence, a smaller fraction of the MSA^- was found in the supermicron size range during ACE-1 ($28 \pm 12\%$ for ACE-1 versus $44 \pm 11\%$ for ACE-2).

The higher supermicron concentration for the ACE-2 marine samples appears to be a result of a longer transport time over the ocean. The ACE-2 marine air masses spent 5 or more days over the ocean prior to reaching the ship. Depending on the location of the ship, the continental ACE-2 air masses spent hours or, at most, 2 days over the ocean prior to being sampled. Likewise, the frontal activity during ACE-1 resulted in relatively short marine boundary layer residence times. It may be that the longer fetch over the ocean during ACE-2 allowed for the accumulation of more MSA^- on the supermicron aerosol through condensation processes.

The occurrence of a more bimodal size distribution for the ACE-2 marine samples agrees with previously reported data for the open ocean and for coastal regions during on-shore flow. Impactor samples collected over the central Pacific and during on-shore flow at the coastal site of Cheeka Peak located on the northwest tip of Washington State showed a bimodal MSA^- size distribution (Pszenny, 1992; Huebert et al., 1993; Quinn et al., 1993). A bimodal distribution also was observed at Sagres during marine conditions although both submicron and supermicron MSA^- concentrations were lower than those measured on the ship. A more prominent submicron mode relative to the supermicron mode was observed in Cheeka Peak samples during northerly winds from Canada and during continental flow at Sagres.

Similarly, MSA^- size distributions from the Gulf of Mexico, Miami, and Peru were not bimodal (Saltzman et al., 1983, 1986; Pszenny et al., 1989).

Submicron and supermicron MSA^- to nss $SO_4^=$ molar ratios for the five source regions in ACE-2 and for Sagres and Punta del Hildalgo are shown in Tables 1 and 2, respectively. Continental ratios for the total aerosol (submicron plus supermicron) from the ship, Sagres, and Punta del Hildalgo averaged 0.019 ± 0.016, 0.01 ± 0.01, and 0.015 ± 0.01, respectively. These values are lower than the continental average of 0.029 ± 0.009 for bulk aerosol measured near the Azores during June of 1992 as part of the ASTEX/MAGE experiment (Huebert et al., 1996). The shipboard marine ratio was 0.21 ± 0.10, a factor of two higher than the Sagres and Punta del Hildalgo values of 0.08 ± 0.12 and 0.10 ± 0.04, respectively. The latter values are lower due to lower MSA^- concentrations. The ASTEX/MAGE marine average also was lower at 0.065 ± 0.005 but because of higher nss $SO_4^=$ concentrations. Variability in the MSA to nss $SO_4^=$ molar ratio is a function of variability in the biogenic source strength of MSA and nss $SO_4^=$ as well as the anthropogenic source of nss $SO_4^=$. The large degree of variability in the ratio observed over NE Atlantic indicates the difficulty of assigning a representative value to a given geographical region.

4.3. *Sea salt aerosol*

Submicron sea salt concentrations measured on the ship for all of ACE-2 ranged from 0.01 to 6.7 $\mu g\, m^{-3}$ with an average and standard deviation of $0.64 \pm 1.0\ \mu g\, m^{-3}$. This is comparable to the ACE-1 average of $1.0 \pm 0.55\ \mu g\, m^{-3}$. Though submicron sea salt concentrations were similar for the two experiments, submicron nss sulfate aerosol concentrations were quite different. For ACE-1, the submicron sea salt to nss sulfate aerosol mass ratio was, on average, 5.3. For ACE-2, the ratio in marine air was 0.72 and in continental air was 0.07. Hence, submicron sea salt had a relatively stronger influence on the aerosol chemical and optical properties during ACE-1.

For the ACE-2 region, there was no obvious correlation of submicron sea salt mass concentration with air mass history (Table 1, Fig. 2). The highest average concentration observed on the ship corresponded to air masses from the Iberian Peninsula ($0.88 \pm 1.5\ \mu g\, m^{-3}$) while one of the lowest corresponded to polar air masses ($0.42 \pm 0.28\ \mu g\, m^{-3}$). Average concentrations measured at Sagres during marine and continental flow were similar and comparable to the lower average values from the ship. Punta del Hildalgo average concentrations for marine and continental conditions also were similar but about half those at Sagres.

In addition, no strong correlation was found between shipboard submicron sea salt concentration and local wind speed. Expressing the dependence of the submicron sea salt mass concentration on local wind speed as

$$\ln(m_{\text{sea salt}}) = aU + \ln b, \tag{2}$$

where $m_{\text{sea salt}}$ is the sea salt mass concentration ($\mu g\, m^{-3}$) and U is local wind speed ($m\, s^{-1}$) results in a coefficient of determination, r^2, of 0.14. The low value of r^2 indicates the importance of factors other than local wind speed in determining the sea salt mass concentration. These include long range transport and vertical mixing (Quinn et al., 1998; Bates et al., 1998). The slope of 0.18 is in good agreement with values previously reported from shipboard measurements in the Pacific (0.16 (Woodcock, 1953)), the Southern Ocean (0.13 (Quinn et al., 1998)), the Atlantic (0.16 (Lovett, 1978)), and the North Sea (0.12 (Marks, 1990)). The low value of r^2 in spite of the fairly consistent slope from region to region indicates that there is a large degree of variance associated with the relationship shown in eq. (2). Hence, the use of eq. (2) to derive the geographical distribution of sea salt mass concentrations may severely underestimate variability in the sea salt aerosol concentration for a given region.

ACE-2 supermicron sea salt concentrations ranged from 1.9 to 18 $\mu g\, m^{-3}$ with an average and standard deviation of $8.6 \pm 3.9\ \mu g\, m^{-3}$. This is about an order of magnitude greater than the submicron average and is comparable to the ACE-1 supermicron average of $9.4 \pm 5.5\ \mu g\, m^{-3}$. Average supermicron concentrations measured at Sagres and Punta del Hildalgo during both marine and continental conditions are comparable to values observed on the ship. Using eq. (2) reveals a similar shipboard sea salt mass–wind speed relationship for the supermicron size range as the submicron size range ($r^2 = 0.20$ and $a = 0.10$).

Sea salt size distributions measured on the ship

for the five source regions are shown in Figs. 3e, f. Distributions from the Iberian Peninsula, the Mediterranean, and Western Europe show a peak in the submicron size range ($0.18 < D_{aero} < 0.31$ μm) that is not observed in the marine distributions of ACE-1 and ACE-2. Peaks in both the submicron and supermicron size range suggest at least two different mechanisms for the production of sea salt aerosol. O'Dowd et al. (1997) observed three distinct sea salt modes and attributed their production to film drops, jet drops, and spume drops.

Sea salt aerosol concentrations were calculated from eq. (1) which prevents the inclusion of non-seasalt K^+, Mg^{+2}, Ca^{+2}, $SO_4^=$, and HCO_3^- in the sea salt mass provided that the assumption that all measured Na^+ was derived from seawater is valid. Given that most of the dust transported from Africa to the North Atlantic occurred at latitudes south of the ship's position (Verver et al., 2000), it is unlikely that African dust provided a strong source of non-sea salt Na^+. Without the measurement of a distinctly crustal element such as Al, however, the possibility that a portion of the submicron sea salt peak was crustal can not be ruled out.

Particulate chloride depletion occurs as H_2SO_4 (or HNO_3) reacts with NaCl in sea salt aerosol to form Na_2SO_4 (or $NaNO_3$) and release gaseous HCl (Clegg and Brimblecombe, 1985). Large losses of particulate chlorine are typically associated with elevated concentrations of anthropogenic combustion products (Keene et al., 1990). The average Cl^- to Na^+ mass ratios measured in air masses from the five regions are shown in Figs. 4a, b as a function of particle size. Also shown is the seawater Cl^- to Na^+ mass ratio of 1.8 which would be the expected ratio if no depletion occurred. Chloride deficits were calculated from

$$\%Cl^- \text{ depletion} = \frac{1.8(Na^+)_{meas} - (Cl^-)_{meas}}{1.8(Na^+)_{meas}} \times 100\% \quad (3)$$

and are listed in Table 3. Chloride deficits in the Atlantic and polar air masses were insignificant relative to the degree of observed variability. Deficits were greater in the continental air masses and significant relative to the observed variability. Deficits on the fourth impactor stage were largest averaging 86 ± 18, 86 ± 17, and $99 \pm 1.1\%$ for the

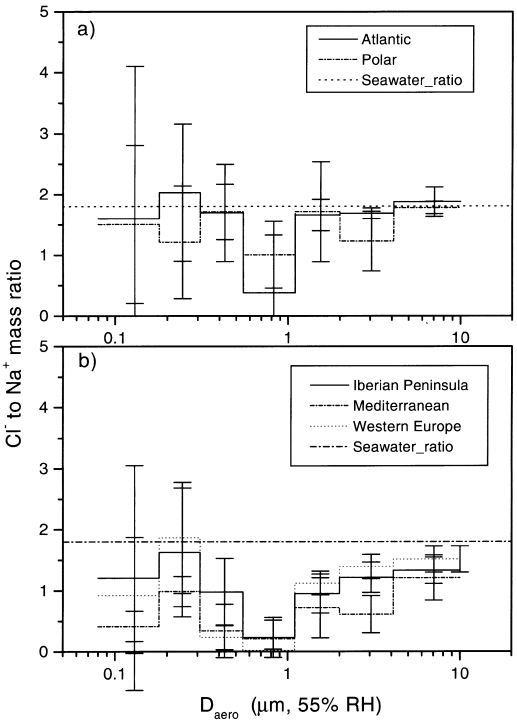

Fig. 4. Average Cl^- to Na^+ mass ratio for the 5 air mass regions as a function of particle size. Also shown is the Cl^- to Na^+ seawater mass ratio of 1.8.

Iberian Peninsula, Mediterranean, and Western European air masses, respectively. Results for the ACE-1 aerosol are similar to the ACE-2 marine aerosol.

4.4. *Carbonaceous aerosol*

A thorough discussion of the carbonaceous aerosol collected during ACE-2 onboard the *Vodyanitskiy* can be found in Novakov et al. (2000). Here, the carbon data are presented to compare average values to the ionic aerosol components. Due to the long times used for collecting aerosol for carbon analysis, no purely marine samples were collected. In addition, no purely Western European samples were collected. For Iberian Peninsula air masses, submicron concentrations of total carbon averaged 1.1 ± 0.47 μg C m^{-3} (Table 1) with about 40% composed of black and 60% composed of organic carbon. Supermicron total carbon concentrations were slightly lower averaging 0.87 ± 0.24 μg C m^{-3}.

Table 3. *Chloride deficit calculated from eq. (3) for the 5 air mass regions as a function of particle size*

	Chloride deficit, %						
Air mass origin	$D_{50,aero}$ 0.18 μm	$D_{50,aero}$ 0.31 μm	$D_{50,aero}$ 0.55 μm	$D_{50,aero}$ 1.1 μm	$D_{50,aero}$ 2.0 μm	$D_{50,aero}$ 4.1 μm	$D_{50,aero}$ 10 μm
Atlantic	-28 ± 140	-21 ± 63	18 ± 45	41 ± 53	10 ± 14	6.0 ± 4.9	-3.7 ± 13
polar	-5.5 ± 74	5.9 ± 51	-0.42 ± 25	32 ± 30	-4.6 ± 46	17 ± 27	1.6 ± 5.6
Iberian Peninsula	36 ± 100	41 ± 59	69 ± 31	86 ± 18	49 ± 18	33 ± 14	26 ± 12
Mediterranean	78 ± 14	49 ± 14	80 ± 24	86 ± 17	64 ± 27	65 ± 17	41 ± 20
western Europe	62 ± 53	24 ± 51	90 ± 11	99 ± 1.1	38 ± 11	24 ± 11	16 ± 12
ACE-1[a]	11 ± 110	42 ± 39	17 ± 24	2.7 ± 17	3.5 ± 21	-9.5 ± 32	10 ± 19

[a] $D_{50,aero}$ for ACE-1 = 0.33, 0.44, 0.76, 1.4, 2.7, 5.6 and 14 μm.

One sample was collected for carbon analysis during Mediterranean flow. Based on this one sample, the total carbon concentration in the submicron size range was 3.9 μg C m^{-3}, about 3.5 times higher than the total carbon observed in the Iberian Peninsula submicron aerosol. Of this, 28% was black carbon and 72% was organic. The supermicron total carbon concentration was 0.96 μg C m^{-3}.

Submicron concentrations of organic carbon measured at Sagres and Punta del Hildalgo under continental flow fell within the range of values measured during Iberian Peninsula flow on the ship. Similarly, black carbon concentrations measured at Sagres during continental flow are similar to the shipboard Iberian Peninsula values. Values measured at Punta del Hildalgo are about a factor of four lower than the shipboard average, however. The shipboard Mediterranean value stands out as being the highest among all continental measurements. Further measurements are needed to determine how representative the shipboard values reported here are of the regional air mass sources.

Supermicron total carbon values during Iberian Peninsula and Mediterranean flow were comparable but about twice that observed during continental conditions at Sagres and Punta del Hildalgo. These were, in turn, about twice the marine values observed at Sagres and Punta del Hildalgo.

Total carbon made up about 11% of the chemically characterized submicron aerosol mass (including sea salt, nss $SO_4^=$ aerosol, MSA^-, and total carbon) in the Iberian Peninsula air masses. During Mediterranean flow, total carbon made up about 35% of the analyzed submicron mass. Supermicron values are 7.5 and 18% for the Iberian Peninsula and Mediterranean, respectively. Including the water associated with the aerosol chemical components at ambient RH and any other chemical species not analyzed will lower this value. In addition, it must be emphasized that the carbon samples were collected over much longer time periods than the ionic samples, adding to the uncertainty in the calculation of the percent mass fractions.

5. Results — aerosol optical properties

5.1. *Aerosol scattering coefficient and hemispheric backscattered ratio*

To separate the scattering coefficient, σ_{sp}, due to submicron and supermicron particles, an impactor ($D_{50,aero} = 1.1$ μm) was valved into the nephclometer sample line at 15-min intervals. This technique was used during both ACE-1 and ACE-2. During ACE-2, the scattering coefficient for the total aerosol ($D_{aero} < 10$ μm) at 550 nm ranged from 5.3 to 160 Mm^{-1}. Values for the submicron and supermicron aerosol ranged from 0.11 to 100 and 1.5 to 67 Mm^{-1}, respectively (Fig. 5). Submicron aerosol dominated scattering by the whole aerosol 45% of the time. This is in contrast to ACE-1 where submicron and supermicron values at 550 nm ranged from 0.66 to 38 and 1.7 to 130 Mm^{-1} with supermicron aerosol being the dominant scatterer throughout the experiment. As sea salt concentrations were comparable for the two experiments, the difference is due to the larger submicron concentrations of non-sea salt chemical components during ACE-2.

Submicron scattering coefficients were similar for Atlantic and polar air masses. Supermicron coefficients also were similar for the two air mass

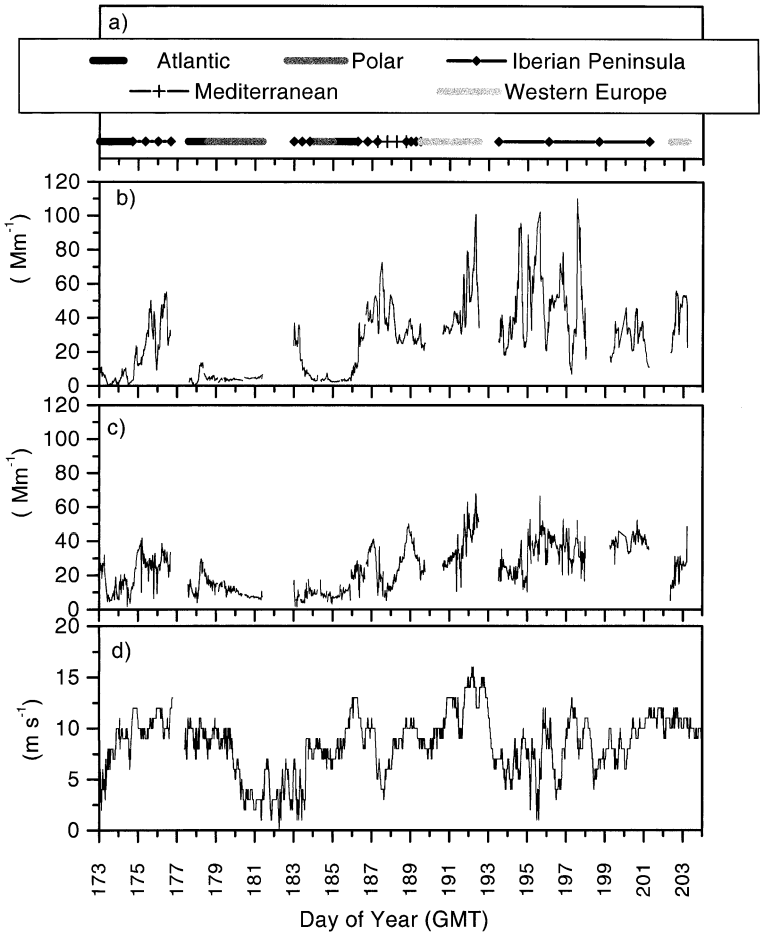

Fig. 5. Shown as a function of day of year throughout the experiment are (a) air mass origin, (b) submicron aerosol scattering coefficient at 550 nm, (c) supermicron aerosol scattering coefficient at 550 nm and (d) wind speed at 10 m asl.

types and were 2.5 to 3 times higher than submicron values due to relatively large supermicron sea salt concentrations. The marine submicron average value is comparable to that observed during ACE-1 as the sum of the nss sulfate and sea salt aerosol is similar for the two experiments. The marine supermicron average value from ACE-1 is slightly higher reflecting higher supermicron sea salt concentrations.

Continental submicron scattering coefficients were about 4 times higher than marine values due, in part, to higher submicron nss sulfate aerosol concentrations. Iberian Peninsula, Mediterranean, and Western European values were comparable. The nss sulfate aerosol size distributions as well as the number size distribution (Bates et al., 2000) differed for each region (Fig. 3b) but a balance between mean diameter and concentration resulted in similar average scattering values.

Continental supermicron scattering coefficients were larger than marine values. Of the continental air masses, Western European and Iberian Peninsula average concentrations were comparable and higher than the Mediterranean average concentration. This corresponds to relatively higher sea salt concentrations in the air masses from Western Europe and the Iberian Peninsula. In addition, a continental source of particles may have contributed to the supermicron scattering that was not accounted for in the chemical

analysis. It is unlikely, however, that African dust was a significant contributor to the measured scattering coefficient. Based on satellite images, transport of dust from Africa to the North Atlantic occurred south of Tenerife (Verver et al., 2000) and, therefore, south of the ship's position. On a few occasions between 9 and 18 July when Tenerife was at the northern edge of the dust plume, weak events were detected at Izana but it is located in the free troposphere.

Low levels of aerosol backscattering and the sensitivity of the nephelometer prevented the derivation of the submicron hemispheric backscattered ratio, $b = \sigma_{bsp}/\sigma_{sp}$, for Atlantic and polar air masses. Of the continental regions, a higher average ratio was observed in the Mediterranean air masses (0.15 ± 0.01) than in the Iberian Peninsula or Western European air masses (0.11 ± 0.02 and 0.11 ± 0.01, respectively) (Table 4). This is a result of the relatively larger concentration of particles at smaller diameters in the submicron size range in the Mediterranean air masses. This can be seen in the nss sulfate aerosol size distribution (Figs. 3a, b) and is confirmed by observations of a dominant submicron mode in the Mediterranean number size distribution centered at 0.105 μm (Bates et al., 2000). This is in contrast to the average Iberian Peninsula number size distribution which had a mode centered at 0.23 μm and the average Western European number size distribution with modes centered at 0.11 and 0.22 μm.

Values of the supermicron hemispheric backscattered ratio were comparable for all air mass regions averaging 0.10 ± 0.03 for the Atlantic and 0.12 ± 0.01 for all other regions. These, in turn, compare well with the ACE-1 average of 0.13 ± 0.01 and indicate the stability of the shape of the sea salt size distribution in the supermicron size range.

5.2. *Spectral dependence of the measured scattering coefficients*

The Ångström exponent, *å*, describes the dependence of the aerosol light scattering coefficient on wavelength and therefore on particle size. Smaller values of å indicate the dominance of larger particles in determining scattering while larger values indicate the opposite. Here, *å* was calculated from the nephelometer-measured σ_{sp} for $D_{aero} < 10$ μm at 550 and 700 nm using

$$å = -\frac{\log[\sigma_{sp}(\lambda)_1/\sigma_{sp}(\lambda)_2]}{\log[\lambda_1/\lambda_2]}. \quad (4)$$

Average values for the five regions are listed in Table 4. In addition, the average spectral dependence of the measured scattering coefficients for the five regions is plotted in Fig. 6.

Values of *å* were lowest for the marine regions averaging 0.16 ± 0.25 for Atlantic air masses and 0.32 ± 0.26 for polar air masses. The ACE-1 average *å* was -0.03 ± 0.38 indicating the dominance of the supermicron size range in controlling the scattering by the aerosol. The nearly neutral spectral dependence for these maritime air masses relative to the continental air masses can be seen in Fig. 6.

Continental values of *å* were larger due to the significant mass concentrations and, therefore,

Table 4. *Aerosol optical properties as a function of air mass origin*

Air mass origin	Sub μm σ_{sp}, 550 nm (Mm^{-1})	Super μm σ_{sp}, 550 nm (Mm^{-1})	Sub μm b, 550 nm	Super μm b, 550 nm	Total *å*, 550, 700 nm	Total σ_{ap}, 550 nm	Total ω_o, 550 nm
Atlantic	4.6 ± 3.4	13 ± 6.9	NA	0.10 ± 0.03	0.16 ± 0.25	0.37 ± 0.22	0.98 ± 0.01
polar	4.0 ± 0.94	10 ± 3.2	NA	0.12 ± 0.01	0.32 ± 0.26	0.37 ± 0.25	0.97 ± 0.02
Iberian Peninsula	37 ± 20	31 ± 11	0.11 ± 0.02	0.12 ± 0.01	1.0 ± 0.39	3.6 ± 3.1	0.95 ± 0.03
Mediterranean	40 ± 14	20 ± 12	0.15 ± 0.01	0.12 ± 0.01	1.5 ± 0.46	7.0 ± 3.3	0.90 ± 0.03
western Europe	44 ± 16	33 ± 13	0.11 ± 0.01	0.12 ± 0.01	1.1 ± 0.26	3.3 ± 1.4	0.96 ± 0.02
ACE-1	4.1 ± 2.8	14 ± 9.7	0.11 ± 0.02	0.13 ± 0.01	-0.03 ± 0.38	0.18 ± 0.27	0.99 ± 0.01

Sub μm = $D_{aero} < 1.1$ μm at 55% RH.
Super μm = 1.1 μm < $D_{aero} < 10$ μm at 55% RH.
Total = $D_{aero} < 10$ μm at 55% RH.
NA = not available.

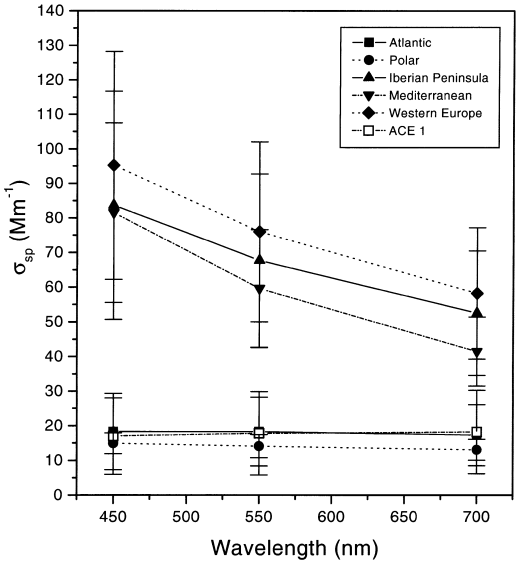

Fig. 6. Nephelometer-measured σ_{sp} as a function of wavelength for the five air mass regions.

scattering coefficients in the submicron size range. Iberian Peninsula and Western European values averaged 1.0 ± 0.39 and 1.1 ± 0.26, respectively. The Mediterranean average å was larger (1.5 ± 0.46) corresponding to a smaller peak diameter in the submicron size range (Bates et al., 2000).

5.3. *Single scattering albedo*

Single scattering albedo, $\omega_o = \sigma_{sp}/(\sigma_{sp} + \sigma_{ap})$, is a measure of the relative magnitude of scattering and absorption by the aerosol. Values reported here are based on the measurement of σ_{ap} and σ_{sp} at 550 nm for $D_{aero} < 10$ μm. During marine flow ω_o ranged from 0.93 to 0.99 with an average of 0.98 ± 0.01 and 0.97 ± 0.02 in Atlantic and polar air, respectively (Table 4). The average ACE-1 value was 0.99 ± 0.01 again indicating the remote nature of the ACE-1 aerosol.

ACE-2 continental values ranged from 0.81 to 0.99. Mediterranean air masses had the lowest average of 0.90 ± 0.03 corresponding to a relatively large black carbon concentration. Average values for the Iberian Peninsula and Western Europe were similar at 0.95 ± 0.03 and 0.96 ± 0.02, respectively.

6. Conclusions

ACE-1 was conducted in the Southern Ocean environment south of Australia and focused on remote marine aerosol minimally perturbed by continental sources. In contrast, ACE-2 was conducted in the NE Atlantic Ocean and studied continental aerosol as it was transported into the marine atmosphere. In addition, the two experiments were conducted in very different meteorological settings. ACE-1 was in a high latitude region of frequent frontal passages while ACE-2 occurred in a mid-latitude region where the synoptic situation is dominated by the position of the Azores High. A comparison of results from the two experiments allows for an assessment of the degree to which continental aerosol perturbs the chemical and optical properties of the marine aerosol system and of the effects on the aerosol of two very different synoptic situations.

Based on back trajectories, a variety of air masses were sampled during ACE-2. Marine air masses came from the central North Atlantic or from north of the Arctic Circle. Continental air masses flowed from the Iberian Peninsula, the Mediterranean, or Western Europe. Based on chemical and optical properties measured during ACE-1 and ACE-2, aerosol in the ACE-2 region was impacted by continental emissions even during periods of marine flow. ACE-2 submicron nss sulfate aerosol concentrations during periods of continental flow were about an order of magnitude larger than concentrations during marine flow. In addition, ACE-2 marine concentrations were about a factor of 4 larger than the ACE-1 average concentration. As a result, even though submicron and supermicron sea salt concentrations were similar for the two experiments, sea salt had relatively less influence on aerosol chemical and optical properties during ACE-2.

The larger nss sulfate concentrations during ACE-2 marine flow relative to ACE-1 also may have resulted from the more stable meteorological conditions which resulted in longer marine boundary layer residence times. A longer time in the boundary layer allows for the accumulation of particle mass through vapor deposition and cloud processing.

During ACE-2 submicron aerosol dominated scattering by the whole aerosol 45% of the time. This is in contrast to ACE-1 where supermicron

aerosol was the dominant scatterer throughout the experiment. This difference resulted in a larger average Ångström exponent for ACE-2 continental aerosol of 1.2 ± 0.26 compared to the ACE-1 average of -0.03 ± 0.38. The ACE-2 marine average was 0.24 ± 0.26. Single scattering albedos also were impacted by continental sources in the ACE-2 region. Average values during ACE-2 continental and marine flow were 0.95 ± 0.03 and 0.98 ± 0.01, respectively, versus 0.99 ± 0.01 for ACE-1. Lowest values corresponded to Mediterranean flow which also had the highest measured black carbon concentrations.

One result common to both the ACE-1 and ACE-2 data sets is the poor correlation between local wind speed and sea salt mass concentration (both submicron and supermicron). Using a log-linear fit between local wind speed and either submicron or supermicron sea salt mass concentration resulted in a coefficient of determination, r^2, of about 0.4 for the ACE-1 data set (Quinn et al., 1998). The same approach resulted in r^2 values of 0.14 and 0.20 for ACE-2 submicron and supermicron sea salt mass, respectively. Local wind speed explains only 10 to 40% of the variance in the measured sea salt concentration. The use of this relationship and consequent dependence on local wind speed to derive distributions of sea salt mass concentrations could significantly underestimate the variability in sea salt concentrations.

7. Acknowledgments

We thank the officers and crew of the *Research Vessel Vodyanitskiy*. This research was funded by the Aerosol Project of the NOAA Climate and Global Change Program and the NOAA Office of Oceanic and Atmospheric Research. Financial support for ship time was provided by the European Commission DG XII (Environment and Climate) and the NOAA Office of Oceanic and Atmospheric Research. This is a contribution to the International Global Atmospheric Chemistry (IGAC) Core Project of the International Geosphere-Biosphere Programme (IGBP) and is part of the IGAC Aerosol Characterization Experiments. This is NOAA PMEL contribution no. 2054 and JISAO contribution no. 649.

REFERENCES

Bates, T. S., Huebert, B. J., Gras, J. L., Griffiths, E. B. and Durkee, P. A. 1998. International Global Atmospheric Chemistry (IGAC) Project's First Aerosol Characterization Experiment (ACE-1): Overview. *J. Geophys. Res.* **103**, 16,297–16,318.

Bates, T. S., Quinn, P. K., Covert, D. S., Coffman, D. J., Johnson, J. E. and Wiedensohler, A. 2000. Aerosol physical properties and controlling processes in the lower marine boundary layer: a comparison of submicron data from ACE-1 and ACE-2. *Tellus* **52B**, 258–272.

Berner, A., Lurzer, C., Pohl, F., Preining, O. and Wagner, P. 1979. The size distribution of the urban aerosol in Vienna. *Sci. Total Environ.* **13**, 245–261.

Clegg, S. L. and Brimblecombe, P. 1985. Potential degassing of hydrogen chloride from acidified sodium chloride droplets. *Atmos. Environ.* **19**, 465–470.

Covert, D. S. 1988. North Pacific marine background aerosols: average ammonium to sulfate ratio equals 1. *J. Geophys. Res.* **93**, 8455–8458.

Dentener, F. J. and Crutzen, P. J. 1994. A 3-dimensional model of the global ammonia cycle. *J. Atmos. Chem.* **19**, 331–369.

Draxler, R. R. 1992. *Hybrid single-particle lagrangian integrated trajectories (HY-SPLIT)*. Version 3.0, User's Guide and Model Description. Tech. Rep. ERL ARL-195, Natl. Oceanic and Atmos. Admin. Silver Spring, Md.

Hainsworth, A. H.W., Dick, A. L. and Gras, J. L. 1998. Climatic context of the First Aerosol Characterization Experiment (ACE-1): a meteorological and chemical overview. *J. Geophys. Res.* **103**, 16,319–16,340.

Hegg, D. A., Covert, D. S. and Kapustin, V. N.. 1992. Modeling a case of particle nucleation in the marine boundary layer. *J. Geophys. Res.* **97**, 9851–9857.

Holland, H. D. 1978. *The Chemistry of the atmosphere and oceans*. John Wiley and Sons, New York, p. 154.

Hoppel, W. A., Frick, G. M., Fitzgerald, J. W. and Larson, R. E. 1994. Marine boundary layer measurements of new particle formation and the effect which nonprecipitating clouds have on the aerosol size distribution. *J. Geophys. Res.* **99**, 14,443–14,459.

Huebert, B. J., Howell, S., Laj, P., Johnson, J. E., Bates, T. S., Quinn, P. K., Yegorov, V., Clarke, A. D. and Porter, J. N. 1993. Observations of the atmospheric sulfur cycle on SAGA 3. *J. Geophys. Res.* **98**, 16985–16995.

Huebert, B. J., Zhuang, L., Howell, S., Noone, K. and Noone, B. 1996. Sulfate, nitrate, methanesulfonate, chloride, ammonium and sodium measurements from ship, island and aircraft during the Atlantic Stratocumulus Transition Experiment/Marine Aerosol Gas Exchange. *J. Geophys. Res.* **101**, 4413–4423.

Keene, W. C., Pszenny, A. A., Jacob, D. J., Duce, R. A., Galloway, J. N., Schultz-Tokos, J. J., Sievering, H. and Boatman, J. F. 1990. The geochemical cycling of reactive chlorine through the marine troposphere. *Global Biogeochem. Cycles* **4**, 407–430.

Lovett, R. F. 1978. Quantitative measurement of airborne sea-salt in the North Atlantic. *Tellus* **30,** 358–363.

Marks, R. 1990. Preliminary investigation on the influence of rain on the production, concentration and vertical distribution of sea salt aerosol. *J. Geophys. Res.* **95**, 22,299–22,304.

Neusüß, C., Weise, D., Birmili, W., Wex, H., Wiedensohler, A. and Covert, D. 2000. Size-segregated chemical, gravimetric and number distribution derived mass closure of the aerosol in Sagres during ACE-2. *Tellus* **52B**, 169–184.

Novakov, T. 1981. Microchemical characterization of aerosols. In: *Nature, aim and methods of microchemistry*. ed. H. Malissa, M. Grasserbauer and R. Belcher. Springer, New York, pp. 141–165.

Novakov, T., Bates, T. and Quinn, P. 2000. Shipboard measurements of concentrations and properties of carbonaceous aerosols during ACE-2.. *Tellus* **52B**, 228–238.

O'Dowd, C. D., Smith, M. H., Consterdine, I. E. and Lowe, J. A. 1997. Marine aerosol, sea-salt and the marine sulfur cycle: a short review. *Atmos. Environ.* **31**, 73–80.

Pszenny, A. A.P. 1992. Particle size distributions of methanesulfonate in the tropical Pacific marine boundary layer. *J. Atmos. Chem.* **14**, 273–284

Pszenny, A. A.P., Castelle, A. J., Duce, R. A. and Galloway, J. N. 1989. A study of the sulfur cycle in the Antarctic marine boundary layer. *J. Geophys. Res.* **94**, 9818–9830.

Putaud, J. P., Van Dingenen, R., Mangoni, M., Virkkula, A., Raes, F., Maring, H., Prospero, J. M., Swietlicki, E., Berg, O. H., Hillamo, R. and Makela, T. 2000. Chemical mass closure and origin assessment of the submicron aerosol in the marine boundary layer and the free troposphere at Tenerife during ACE-2 *Tellus* **52B**, 141–168.

Quinn, P. K., Covert, D. S., Bates, T. S., Kapustin, V. N., Ramsey-Bell, D. C. and McInnes, L. M.. 1993. Relationships between size-resolved particulate non-seasalt sulfate, methanesulfonate and ammonium mass and number concentration. *J. Geophys. Res.* **98**, 10411–10427.

Quinn, P. K., Charlson, R. J. and Bates, T. S. 1988. Simultaneous observations of ammonia in the atmosphere and ocean. *Nature* **335**, 336–338.

Quinn, P. K., Coffman, D. J., Kapustin, V. N., Bates, T. S. and Covert, D. S. 1998. Aerosol optical properties in the marine boundary layer during the first Aerosol Characterization Experiment (ACE-1) and the underlying chemical and physical aerosol properties. *J. Geophys. Res.* **103**, 16,547–16,563.

Saltzman, E. S., Savoie, D. L., Zika, R. G. and Prospero, J. M. 1983. Methane sulfonic acid in the marine atmosphere. *J. Geophys. Res.* **88**, 10,897–10,902

Saltzman, E. S., Savoie, D. L., Prospero, J. M. and Zika, R. G. 1986. Elevated atmospheric sulfur levels off the Peruvian coast. *J. Geophys. Res.* **91**, 7913–7918.

Verver, G., Raes, F., Vogelezang, D. and Johnson, D. 2000. The second Aerosol Characterization Experiment (ACE-2): Meteorological and chemical context. *Tellus* **52B**, 126–140.

Whittlestone, S., Gras, J. L. and Siems, S. T. 1998. Surface air mass origins during the First Aerosol Characterization Experiment. *J. Geophys. Res.* **103**, 16,341–16,350.

Whittlestone, S. and Zahorowski, W. 1998. Baseline radon detectors for shipboard use: development and deployment in the first aerosol characterization experiment (ACE-1). *J. Geophys. Res.* **103**, 16,743–16,752.

Woodcock, A. H. 1953. Salt nuclei in marine air as a function of altitude and wind force. *J. Meteorol.* **10**, 362–371.